Development 130, 3557-3565

doi:10.1242/dev.00586

Macrophage-mediated corpse engulfment is required for normal *Drosophila* CNS morphogenesis

Heather C. Sears, Caleb J. Kennedy and Paul A. Garrity*

Department of Biology, Massachusetts Institute of Technology, 77 Massachusetts Avenue 68-230B, Cambridge, MA 02139, USA
*Author for correspondence (e-mail: pgarrity@mit.edu)

Accepted 8 May 2003

SUMMARY

Cell death plays an essential role in development, and the removal of cell corpses presents an important challenge for the developing organism. Macrophages are largely responsible for the clearance of cell corpses in *Drosophila melanogaster* and mammalian systems. We have examined the developmental requirement for macrophages in *Drosophila* and find that macrophage function is essential for central nervous system (CNS) morphogenesis. We generate and analyze mutations in the *Pvr* locus, which encodes a receptor tyrosine kinase of the PDGF/VEGF family that is required for hemocyte migration. We find that loss of *Pvr* function causes the mispositioning of glia within the CNS and the disruption of the CNS axon scaffold. We further find that inhibition of hemocyte development or of Croquemort, a receptor required for macrophage-mediated corpse engulfment, causes similar CNS defects. These data indicate that macrophage-mediated clearance of cell corpses is required for proper morphogenesis of the *Drosophila* CNS.

Key words: Pvr, Engulfment, Hemocyte, Cell death, Apoptosis, *Drosophila*

INTRODUCTION

Programmed cell death plays an important role in sculpting tissues and neuronal circuitry during development (Jacobson et al., 1997). In *Drosophila melanogaster*, large numbers of cells die during development, and these deaths serve to shape tissue, to delete unnecessary structures, to control cell numbers and to eliminate damaged or developmentally defective cells (Abrams, 2002; Baehrecke, 2002; Bangs and White, 2000). For example, activation of cell death is essential for sculpting the embryonic head (Lohmann et al., 2002), eliminating cells at metamorphosis (Jiang et al., 1997), limiting the divisions of post-embryonic neuroblasts (Bello et al., 2003) and specifying the precise number of neurons in each cartridge within the lamina ganglion of the visual system (Huang et al., 1998). Such widespread occurrence of cell death creates many cell corpses, and the engulfment and removal of cell corpses is a prominent feature of animal development (Fadok and Chimini, 2001).

Macrophages are responsible for the majority of cell corpse removal during mammalian development (Hopkinson-Woolley et al., 1994; Hume et al., 1983; Morris et al., 1991). In *Drosophila*, cell corpse removal also relies on specialized phagocytic cells that resemble mammalian macrophages in a number of cellular and molecular properties (Franc, 2002). *Drosophila* macrophages are derived from hematopoietic precursor cells known as hemocytes, which differentiate into macrophages displaying phagocytic and scavenger properties in response to cell corpse exposure (Tepass et al., 1994). Work on mammalian macrophages and other phagocytic cells has identified several classes of receptors implicated in corpse recognition, including lectins, integrins, the MER tyrosine kinase, the phosphatidylserine receptor (PSR) and scavenger receptors such as CD36 (Fadok and Chimini, 2001). *Drosophila* macrophages express a CD36-related receptor, Croquemort (Franc et al., 1996), and *croquemort* (*crq*) function is required for macrophages to take up dead cells efficiently in the developing embryo (Franc et al., 1999).

As macrophages are responsible for much of the dead cell engulfment in developing animals, an important role for macrophages in tissue morphogenesis during development has been suggested (Morris et al., 1991). However, direct evidence of a required role for macrophage-mediated cell corpse engulfment in development is limited. In the feet of PU.1 mutant mice that lack macrophages, for example, other cell types take over the engulfing role and permit morphogenesis to proceed, albeit at a slower pace (Wood et al., 2000). By contrast, in the developing mouse retina macrophages are essential for cell death-mediated morphogenesis (Lang et al., 1994; Lang and Bishop, 1993). In this case, the primary defect is not caused by a failure of engulfment. Rather, macrophages are required to initiate the cell deaths that normally eliminate the hyaloid vessels and the pupillary membrane during the development of the mouse eye.

In the CNS of *Drosophila melanogaster* embryos, programmed cell death eliminates many neurons and glia (Jacobs, 2000; Sonnenfeld and Jacobs, 1995b). In the case of the midline glia, approximately ten midline glial cells are generated in each segment by stage 13 of embryonic

development. As development proceeds, most of these glia are eliminated by programmed cell death, leaving two to three midline glia per segment by stage 17 (Klambt et al., 1991; Sonnenfeld and Jacobs, 1995a; Zhou et al., 1995). Recent work indicates that midline glial cell survival is mediated through activation of MAP kinase signaling in the midline glia via the reception of the EGFR ligand Spitz, which is provided by the developing neurons (Bergmann et al., 2002). In addition to midline glia, a subset of developing neurons and longitudinal glia (which flank the midline) are also removed through cell death (Hidalgo et al., 2001; Sonnenfeld and Jacobs, 1995b). Electron microscopic studies by Sonnenfeld and Jacobs demonstrated that the majority of cell corpses are expelled from the CNS and engulfed by macrophages (Sonnenfeld and Jacobs, 1995b). Cell corpses can also be detected in glial cells both within and at the surface of the CNS, indicating that glial cells also contribute to removal of dead cells. These authors also examined macrophage-less embryos derived from *Bic-D* mothers and found an increase in the number of unengulfed cells within the CNS as well as increased numbers in subperineurial glial cells at the periphery of the CNS. However, embryos derived from *Bic-D* mutant mothers have widespread patterning defects (duplication of posterior structures at the expense of anterior structures), complicating analysis of the consequences of macrophage loss on development.

Pvr encodes the *Drosophila* member of the vertebrate PDGF/VEGF receptor tyrosine kinase family (Duchek et al., 2001; Heino et al., 2001). *Pvr* was initially shown by Duchek et al. to regulate border cell migration during oogenesis (Duchek et al., 2001) and subsequently shown by Cho et al. to control hemocyte migration (Cho et al., 2002). Cho et al. found that hemocytes fail to disperse normally in *Pvr* mutant animals and that expression of the Pvr ligand Pvf2 in an ectopic location can attract hemocytes to the site of Pvf2 expression (Cho et al., 2002). We independently isolated mutations in *Pvr* and have used our analysis of *Pvr* as a starting point to investigate the previously unexplored function of hemocytes in CNS development.

In this work, we use a combination of gene targeting by homologous recombination and chemical mutagenesis to create mutations in *Pvr*. We find that *Pvr* mutations, which disrupt hemocyte migration, cause defects in the patterning of the CNS axon scaffold and the positioning of CNS glia without affecting the pattern of midline glial cell death. We further find that *serpent* (*srp*) mutant animals (which lack hemocytes) and animals in which the function of the macrophage scavenger receptor Croquemort has been inhibited both show defects in CNS patterning similar to those of *Pvr* mutants. Taken together, these data suggest that macrophage-mediated engulfment is necessary for proper *Drosophila* CNS development.

MATERIALS AND METHODS

Genetics and molecular biology

Fly stocks and plasmids for creating the Pvr disruption allele were obtained from K. Golic. To create the targeting construct, bases 125741-130091 from AE003620 were excised as a *Sac*II/*Sgr*AI fragment and cloned into pTV2. An I-*Sce*I recognition site was inserted at the *Bst*EII site at base 128126. Targeting was done as described (Rong and Golic, 2000). EMS alleles were sequenced by the MGH DNA Sequencing Core Facility.

Genomic DNA was prepared for long-range PCR by crushing single flies (Canton-S, *Pvr* knock-out donor, or heterozygous *Pvr* knock-out) in 50 μl squishing buffer (10 mM Tris-HCl pH 8.2, 1 mM EDTA, 25 mM NaCl, 200 μg/ml Proteinase K). Crushed flies were incubated at 37°C for 30 minutes and Proteinase K was inactivated at 95°C for 2 minutes. Long-range PCR was performed using the Expand Long Template PCR System (Roche). Primers used to confirm homologous recombination were 5′-AATCGTACCGTTGCGAATA-AGTGGG-3′ (Primer A), 5′-AGAAGCGAGAGGAGTTTTGGC-ACAGC-3′ (Primer B), 5′-TTTGTTCGACGACCTTGGAGCGAC-3′ (Primer C) and 5′-TGGATAAAGTTCCATCACCACCACGG-3′ (Primer D). Control PCR was performed with primers against Pvr genomic DNA, 5′-CAGTGCAACGCTAAGTGAGCC-3′ and 5′-TC-TTCACGCAATAGTAGGCTGCC-3′.

The following fly stocks were kindly provided by those indicated: *slit(1.0)-lacZ* (I. Rebay), *Sim-Gal4* (C. Goodman), *Gcm-Gal4* (U. Tepass), *UAS-Pvr^{DN}* (P. Rorth), *srp^{neo45}* (U. Banerjee) and *Df(3L)H99* (Bloomington Stock Center). Homozygous *Pvr* and *srp^{neo45}* mutant embryos were identified through the use of balancers marked with GFP (Bloomington Stock Center).

Southern blotting

Genomic DNA isolated from 25 Canton-S or *Pvr^{KO}/CyO* flies was digested with *Pvu*II. Digested DNAs were electrophoresed on an 0.8% agarose gel and transferred by downward capillary transfer to a Zeta-Probe GT membrane (BioRad). Membrane was subsequently treated following manufacturer's protocol. The probe template was amplified by PCR using genomic DNA and primers 5′-ATCGCTCGTATGCC-CTACAACG-3′ and 5′-CTTCCTGTCAACAATCGCACATTC-3′, which span 776 bases of the Pvr locus. ^{32}P-labelled probe was made from this template using the DECAprime II Kit (Ambion).

Immunohistochemistry and western blotting

All embryos were stained as described (Patel, 1994) using: rat polyclonal antiserum against Repo (Campbell et al., 1994) (1:500); mouse monoclonal antibody against *lacZ* (1:100; Promega); mouse polyclonal antiserum against Peroxidasin (Nelson et al., 1994) (1:500) and rabbit polyclonal antiserum against Croquemort (Franc et al., 1999) (1:500). The mouse monoclonal antibodies BP102 and 1D4, developed by C. Goodman, were obtained from the Developmental Studies Hybridoma Bank developed under the auspices of the NICHD and maintained by The University of Iowa, Department of Biological Sciences, Iowa City, IA 52242. Secondary antibodies labeled with HRP, FITC or Cy3 were obtained from Jackson Laboratories. Polyclonal antiserum against Pvr was produced in rats (Covance) against a 30 kDa peptide containing the 275 C-terminal amino acids of Pvr fused to a 6XHis tag. Anti-Pvr antiserum was used at 1:300 on embryos. Fluorescent images were obtained using a Nikon PCM2000 confocal microscope.

For each lane of western blots, 10 embryos of each genotype were homogenized in phosphate-buffered saline (PBS) (130 mM NaCl, 175 mM Na_2HPO_4, 60 mM NaH_2PO_4). Lysates were run on a 9% polyacrylamide gel and transferred to Hybond-P membrane (Amersham Pharmacia). Membranes were blocked in 5% nonfat milk and probed with anti-Pvr antisera diluted 1:2000 and HRP-conjugated goat anti-rat antibody diluted at 1:5000. Blots were stripped and reprobed with rat monoclonal antibody against Elav to confirm that each *Pvr* mutant lane contained similar or greater amounts of total protein than wild-type control.

RNAi

Inhibition of Crq by RNAi was performed as described (Kennerdell and Carthew, 1998). Bases 681-1203 and 1209-1737 of Crq cDNA RE02070 (ResGen; GenBank Accession Number AY070904) were PCR-amplified using primer 5′-GAATTAATACGACTCACTATA-

GGGAGAGGGACTGATGCCTATGAAAGCTG-3′ with 5′-GAATTAATACGACTCACTATAGGGAGAAGCCATCGTAAGTCAGCGACTC-3′ and 5′-GAATTAATACGACTCACTATAGGGAGAACTATTCACACGGGCACTGACG-3′ with 5′-GAATTAATACGACTCACTATAGGGAGATAATCTGGATGCGTCCATGCAC-3′. The 5′-end of each oligonucleotide contains a T7 RNA polymerase promoter sequence. dsRNAs were synthesized with T7 RNA polymerase from the MEGAscript High Yield Transcription Kit (Ambion). dsRNA was injected into Canton-S embryos at 1 μg/μl. Both Crq dsRNAs gave similar results. Control embryos injected with dsRNA from the Gal4 gene or Ptp99A gave no detectable phenotype.

RESULTS

Targeted disruption of the *Pvr* locus

To initiate our studies of *Pvr* function, the *Pvr* locus was disrupted using a recently described procedure for gene disruption by homologous recombination (Fig. 1A) (Rong and Golic, 2000; Rong and Golic, 2001). Ten independent homologous recombination events were recovered from the progeny of 3000 females, and the products of the targeting events were examined by a combination of long-range PCR and Southern blotting. Nine out of ten targeted insertions, including Pvr^{KO2}, yield the products expected for a successful targeting event in both PCR and Southern blot analysis (Fig. 1B,C). These alleles all failed to complement the lethality of *Df(2L)TE128x11*, a chromosomal deficiency that removes *Pvr*, completing embryogenesis but failing to hatch. One targeted insertion allele, Pvr^{KO8}, appeared to have undergone a complex combination of DNA insertion and duplication and was not analyzed further.

In addition to creating targeted insertions at the *Pvr* locus, we identified multiple *Pvr* alleles though a genetic non-complementation screen. Nine-thousand eight-hundred and ten lines of EMS-mutagenized flies were screened for failure to complement the lethality of *Df(2L)TE128x11*. One-hundred and eighty-five lethal or semi-lethal lines were recovered, of which 20 failed to complement Pvr^{KO} lethality. Among these putative *Pvr* alleles, we have identified four that carry missense mutations in the extracellular domain, four that create stop codons in the extracellular domain and three that carry missense mutations in the kinase domain (Fig. 2A). The mutations in the kinase domain disrupt residues highly conserved among protein kinases (Hanks et al., 1988; Johnson et al., 1996). In Pvr^{729} an alanine residue in the catalytic loop, highly conserved among tyrosine kinases, is changed to a

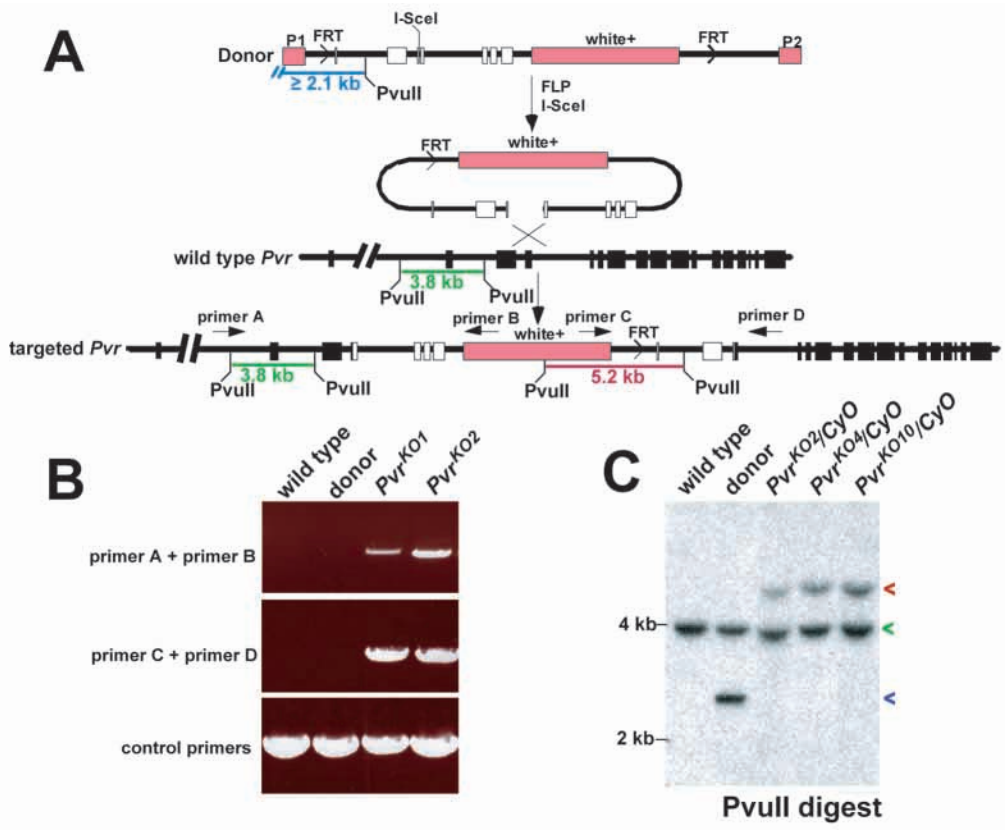

Fig. 1. Disruption of the *Pvr* locus through homologous recombination-mediated gene targeting. (A) A P-element containing 4.5 kb of *Pvr* genomic sequence, a mini-white gene and FRT sequences was randomly inserted by transposition onto the third chromosome. This DNA was circularized through expression of FLP recombinase and linearized through expression of the yeast restriction endonuclease I-*Sce*I. This linear fragment recombined with the endogenous *Pvr* locus to produce two tandem partial copies of the *Pvr* gene. White boxes indicate exons that originate from the donor fragment. Black boxes indicate exons that originate from the endogenous locus. (B) PCR analysis of homologous recombinants using the primer pairs indicated in A. One primer of each pair anneals to DNA in the mini-white gene in the targeting construct, while the other primer of each pair anneals to genomic DNA from the endogenous locus. In the top panel, primers A and B were used to amplify DNA to the left of the mini-white gene. In the center panel, primers C and D were used to amplify DNA to the right of the mini-white gene. As expected, DNA from wild-type flies or flies with the donor P-element yield no PCR product in either case. DNA from homozygous *Pvr* knock-out embryos gives the expected size PCR products. In the bottom panel, control primers were used to amplify a fragment from the same genomic DNA used in the top and center panels. (C) Southern blot analysis of homologous recombinants. The locations and sizes of the fragments recognized by the probe are indicated in A. Red arrowhead, homologous recombinant-specific band; green arrowhead, endogenous *Pvr* locus band; blue arrowhead, pre-recombination donor-specific band. As Pvr^{KO2}, Pvr^{KO4}, and Pvr^{KO10} are homozygous lethal early in development, DNA was obtained from adults heterozygous for each Pvr^{KO} allele and a wild-type copy of *Pvr* on a CyO chromosome. As expected, the endogenous *Pvr* locus band (green) is approximately twice as intense as the homologous recombinant-specific band (red), because the endogenous *Pvr* locus band is generated from both alleles.

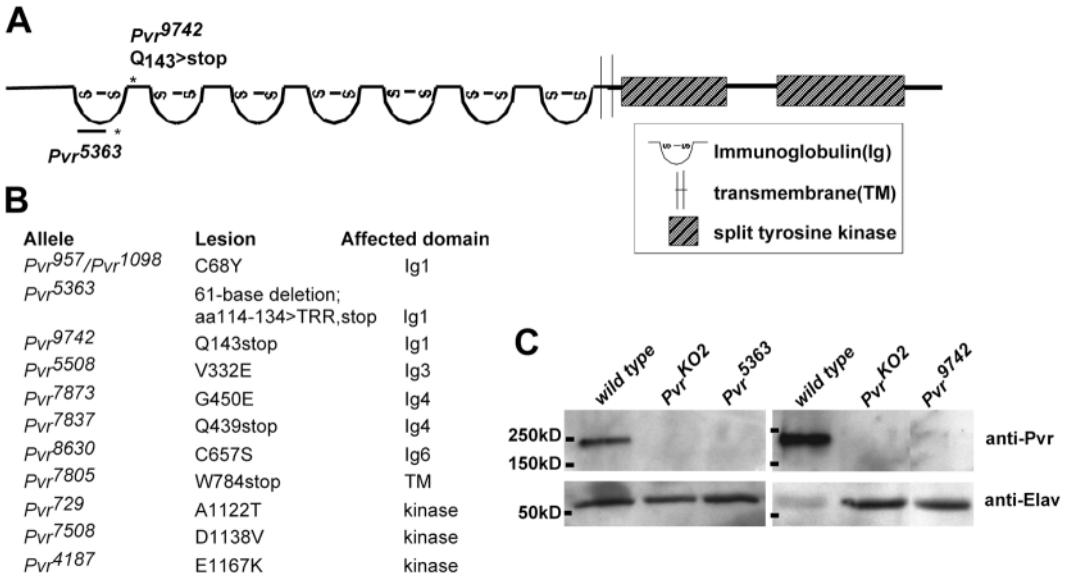

Fig. 2. *Pvr* alleles generated by EMS mutagenesis. (A) Schematic of the Pvr proteins noting the location of lesions predicted to severely truncate the Pvr protein. In Pvr^{9742}, Q143 is converted to a stop codon. In Pvr^{5363}, a 61-base deletion results in the deletion of amino acids 114-134 and a subsequent frameshift that results in three new amino acids and a stop codon. (B) Molecular lesions in *Pvr* alleles. Four alleles truncate the protein, four alleles contain missense mutations in the extracellular domain and three contain missense mutations in the kinase domain. (C) Western blots containing protein from the genotypes indicated probed with anti-Pvr antiserum. A single major protein species is detected in wild-type flies. This species cannot be detected in the *Pvr* mutants. Blots were reprobed with anti-Elav antiserum to confirm that similar or greater levels of protein were present in mutant lanes compared with wild-type controls.

threonine. In Pvr^{4187} a glutamate residue in the activation loop, highly conserved among all protein kinases, is changed to a lysine. Finally, in Pvr^{7508} an aspartate residue in the DFG motif at the base of the activation loop is changed to a valine. Crystallographic data indicates this residue is involved in the divalent cation binding that contributes to nucleotide triphosphate recognition (Johnson et al., 1996). The recovery of these changes in the kinase region are consistent with the importance of catalytic activity for *Pvr* function. All 11 of these EMS-induced *Pvr* alleles behave as embryonic lethal mutations.

We have focused our analysis on three alleles predicted to yield severely truncated *Pvr* proteins. Pvr^{KO2} contains two truncated copies of *Pvr*: one copy encodes a Pvr protein truncated after the fourth Ig domain; the other copy lacks promoter sequences and predicted start codons. Pvr^{9742} contains a stop codon immediately after the first Ig domain, while Pvr^{5363} has a 61-base deletion that removes amino acids 114-134 from the first Ig domain and replaces them with three new residues and a stop codon. Stage 16/17 Pvr^{KO2}, Pvr^{9742} and Pvr^{5363} embryos were examined for Pvr protein expression by western blot using antisera raised against the C-terminal 275 amino acids of Pvr. Pvr expression was not detected in any of these mutant animals (Fig. 1C). This was the case even when lanes containing protein derived from *Pvr* mutant embryos contained substantially more total protein than lanes containing protein from wild-type control embryos, as assessed by reprobing the blots with a monoclonal antibody against the pan-neuronal protein Elav (Fig. 1C). Pvr^{KO2}, Pvr^{9742} and Pvr^{5363} give equivalent results in the studies described below.

Pvr is required for proper CNS axon scaffold formation and glial positioning

We next examined CNS patterning in *Pvr* mutants. CNS axons in the *Drosophila* embryo establish a precise pattern reiterated in each segment (Fig. 3A). CNS axons establish two longitudinal tracts that run the length of the embryo on either side of the midline, with a subset of these axons crossing the midline of the embryo, forming two commissural axon bundles per segment. CNS axons are guided in part by signals from glia precisely positioned at the midline and along the longitudinal tracts (Hidalgo and Booth, 2000a; Kidd et al., 1999). Although CNS axon architecture was grossly normal in *Pvr* mutants, the precise ladder-like axon scaffold seen in wild-type embryos was disrupted (Fig. 3B). The scaffold in each segment had a rounded appearance, owing to changes in the separation between the anterior and posterior commissures and the longitudinal tracts.

As a metric of CNS shape change in *Pvr* mutants, we calculated the ratio of the distance between the longitudinal tracts in each segment of late stage 16 embryos to the distance between anterior and posterior commissures. As shown in Table 1, this ratio was significantly smaller in *Pvr* mutants than in wild-type or *Pvr* heterozygote controls (unpaired *t*-test, $P<0.01$).

As glial cells within the CNS are required for proper axon tract formation, we examined the positioning of glial cells in *Pvr* mutants. Many CNS glial cells express the homeobox protein Repo and require Repo for their proper development (Campbell et al., 1994; Halter et al., 1995). Repo-expressing glia form a patterned array along the longitudinal axon tracts and are largely excluded from the midline, except for a thin line of glia that enter the midline in each embryonic segment (Campbell et al., 1994; Jacobs and Goodman, 1989) (Fig. 3C, arrowhead). In *Pvr* mutants, however, large numbers of Repo-positive glia accumulated in the midline (Fig. 3D, arrowheads). Thus, *Pvr* mutants have defects in both CNS axon tract morphology and glial positioning.

As *Pvr* mutants showed disruptions in CNS axon tract shape and glial cell positioning near the CNS midline, the pathfinding

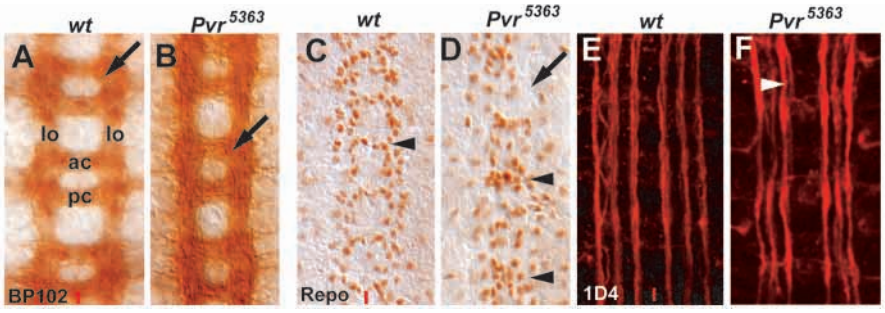

Fig. 3 *Pvr* is required for proper CNS morphogenesis. (A,B) Stage 16 (A) wild-type (Canton-S) and (B) Pvr^{5363} embryos stained with MAb BP102 to visualize CNS axons. ac, anterior commissure. pc, posterior commissure. lo, longitudinal tracts. Red line, CNS midline. In wild type, the commissures and longitudinal tracts form a rectangular axon scaffold in each segment (arrow), whereas in *Pvr*, the longitudinal tracts are closer together than in wild type, giving the axon scaffold a rounded appearance in each segment (arrow). (C,D) Stage 16 (C) wild type (Canton-S) and (D) Pvr^{5363} embryos stained with anti-Repo to visualize glia. In wild type, Repo-positive glia are arranged in a patterned array along the two longitudinal tracts, with a single row of Repo-positive glia between the longitudinal tracts in each segment (arrowhead). In *Pvr* mutants, Repo-positive glia accumulate at the midline (arrowheads), and there are fewer Repo-positive glia in the longitudinal tract region (arrow). The longitudinal tracts appear in outline in the photograph, which was taken using differential interference contrast (DIC) optics. (E,F) Longitudinal axon tracts of stage 17 embryos are stained with the anti-Fasciclin 2 monoclonal antibody 1D4. (E) Wild type. Three tightly bundled axon tracts can be seen on each side of the midline. (F) Pvr^{5363} mutants also form three axon tracts on either side of the midline. No ectopic axon crossing of the midline can be detected, although minor defasciculation of axon tracts can be seen in some segments (arrowhead).

of CNS axons near the midline in *Pvr* mutants was examined in greater detail. The monoclonal antibody 1D4 (mAb 1D4) recognizes the Fasciclin 2 protein (Van Vactor et al., 1993) and labels a subset of longitudinal bundles that grow adjacent to the CNS midline. Mab1D4 is a commonly used tool for assessing axon fasciculation patterns and detecting inappropriate axon crossing of the CNS midline (Hidalgo and Brand, 1997; Kidd et al., 1998; Lin et al., 1994). Despite the changes in CNS axon scaffold shape and longitudinal glial distribution observed in *Pvr* mutants, no inappropriate axon crossing of the midline was detected (Fig. 3E,F). In addition, in wild-type animals three major tracts of Fasciclin 2-positive axons are observed near the dorsal surface of the CNS on either side of the midline (Fig. 3E). Three major tracts of Fasciclin 2-positive axons were also observed in *Pvr* mutants (Fig. 3F).

Table 1. Quantitative representation of CNS commissure morphology of late stage 16/early stage 17 embryos

Genotype	Ratio of distance between longitudinals and commissures*
+/+	2.5±0.09 (*n*=40)
Pvr^{KO2}/+	2.6±0.09 (*n*=40)
Pvr^{KO2}	1.6±0.06† (*n*=40)
Pvr^{5363}	1.7±0.07† (*n*=32)
srp^{neo45}	1.6±0.08† (*n*=40)
crq RNAi	1.8±0.07† (*n*=32)

*In each embryonic segment, the distance between the longitudinal axon bundles and the distance between the commissural axon bundles was measured, and the ratio of the two quantities was calculated. A ratio was used so that variations in overall embryo size between individuals would not contribute to the result. Error is given as standard error of the mean.

†Significantly different from wild type, $P<0.01$ (unpaired *t*-test).

n=number of segments quantitated.

Although these tracts were relatively normal, they did show very mild defasciculation in some segments, with axons in *Pvr* mutants occasionally separating from one another by greater distances than normal (Fig. 3F). As disruptions in longitudinal glial cell development disrupt the formation of these axon bundles (Hidalgo and Booth, 2000b), the minor axon tract defects observed in *Pvr* mutants were not unexpected given the glial cell mispositioning seen in *Pvr* mutants (Fig. 3D).

Pvr functions in hemocytes

To investigate the source of the CNS defects in *Pvr* mutants, we identified the cell populations expressing Pvr. Pvr protein was detected on several cell populations during embryonic development. In stage 16 embryos, Pvr was prominently expressed by cells at the surface of the embryo, as well as by cells scattered throughout the embryo and by cells at the CNS midline (Fig. 4A). The large number of Pvr-expressing cells scattered throughout the embryo were hemocytes, as they co-expressed the hemocyte marker Peroxidasin (Fig. 4B-D). The Pvr-expressing cells at the CNS midline were midline glia (a population distinct from the Repo-positive glia mentioned above) and were intimately associated with the CNS commissures (Fig. 4E,F). Pvr expression could not be detected in Pvr^{KO2}, Pvr^{5363} or Pvr^{9742} embryos, confirming the specificity of the antiserum (Fig. 4G).

Drosophila midline glia play important roles in separating and wrapping CNS axon commissures (Jacobs, 2000). Although midline glia expressed Pvr and *Pvr* mutants exhibited defects in commissure morphology, we could detect no role for Pvr in the midline cells. We first examined the number of midline glia present in *Pvr* mutant embryos using the midline glial marker *sli(1.0)-lacZ* (Nambu et al., 1991). Wild-type stage 17 embryos contained 2.8±0.2 glia per segment (*n*=18;±s.e.m.), while Pvr^{KO2} embryos contained 2.7±0.2 glia per segment (*n*=25). Thus, there was no detectable alteration in the number of midline glia. Midline glial cell development was further examined by staining for Wrapper, an immunoglobulin superfamily protein specifically expressed in midline glia and required for midline glial survival (Noordermeer et al., 1998). Wrapper was appropriately expressed by midline glia in *Pvr* mutants (Fig. 5A,B). To test directly whether *Pvr* acted in midline glia, high-level expression of a dominant-negative form of Pvr (Duchek et al., 2001) was driven in all midline cells using the *Sim:Gal4* driver or specifically in midline glia using the *Slit:Gal4* driver. However, in neither case was a detectable CNS axon or Repo-positive glia phenotype generated (Fig. 5C,E; H.C.S., C.J.K. and P.A.G., unpublished).

We next examined whether the CNS phenotype was related to Pvr expression in hemocytes. In the *Pvr* alleles recovered in our studies, hemocytes largely failed to migrate away from

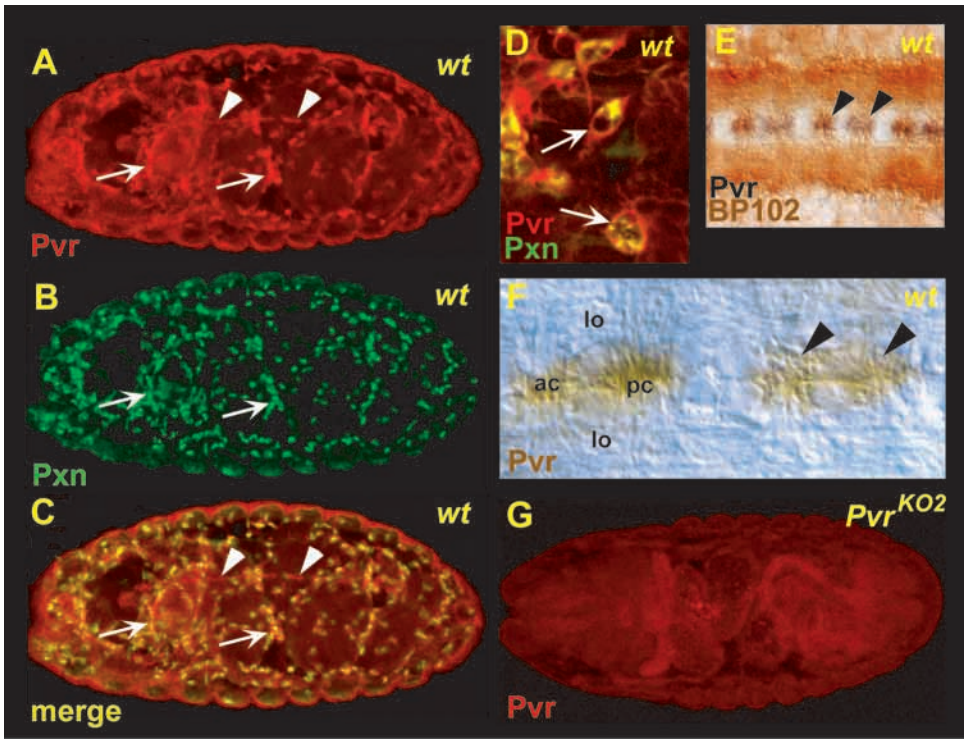

Fig. 4. Pvr protein is present on midline glia and hemocytes. (A-D) Wild-type stage 16 embryo stained with anti-Pvr (red) and anti-Peroxidasin (Pxn) (green). Yellow indicates overlap in the merged images (C,D). Pvr protein can be detected at the midline (arrowheads), in hemocytes (arrows) and at the surface of the embryo. (D) Higher magnification image of embryo depicted in A-C. The expression of Pvr in hemocytes is confirmed by co-expression with Peroxidasin in C and D. (E) Stage 17 embryo double-labeled with anti-Pvr (black) and BP102 (brown). Pvr protein is expressed on midline glia that surround the CNS commissures (arrowhead). (F) Higher magnification image of wild-type stage 16 embryo stained with anti-Pvr. CNS axon tracts are visualized using DIC optics. Pvr protein is expressed on midline glia (arrowheads) that surround the anterior and posterior CNS commissures. ac, anterior commissure. pc, posterior commissure. lo, longitudinal axons tracts. (G) Pvr^{KO2} mutant embryo stained with anti-Pvr. Anti-Pvr staining cannot be detected in mutant animals.

their birthplace in the head (Fig. 5G,H), consistent with the recent observations of Cho et al. (Cho et al., 2002). To test whether Pvr function in hemocytes was important for CNS development, we drove expression of dominant-negative Pvr in the developing hemocytes. While no solely hemocyte-specific Gal4 driver is available, *Gcm:Gal4* has been used previously to drive gene expression in embryonic hemocytes (Cho et al., 2002). We find that *Gcm:Gal4* drives gene expression specifically in hemocytes beginning at stage 11 and later, beginning at stage 15, in other cells that do not detectably express Pvr (H.C.S., C.J.K. and P.A.G., unpublished). Embryos expressing dominant-negative Pvr under the control of *Gcm:Gal4* had hemocyte migration defects resembling those of *Pvr* mutants, consistent with *Pvr* acting cell-autonomously to control hemocyte migration (Fig. 5I). Most importantly, embryos expressing dominant-negative Pvr under *Gcm:Gal4* control also exhibited rounding of CNS axon commissures and mispositioning of Repo-positive glial cells similar to *Pvr* mutants (Fig. 5D,F). These data are consistent with Pvr acting in hemocytes to control CNS patterning and suggest that hemocyte function is required during CNS development.

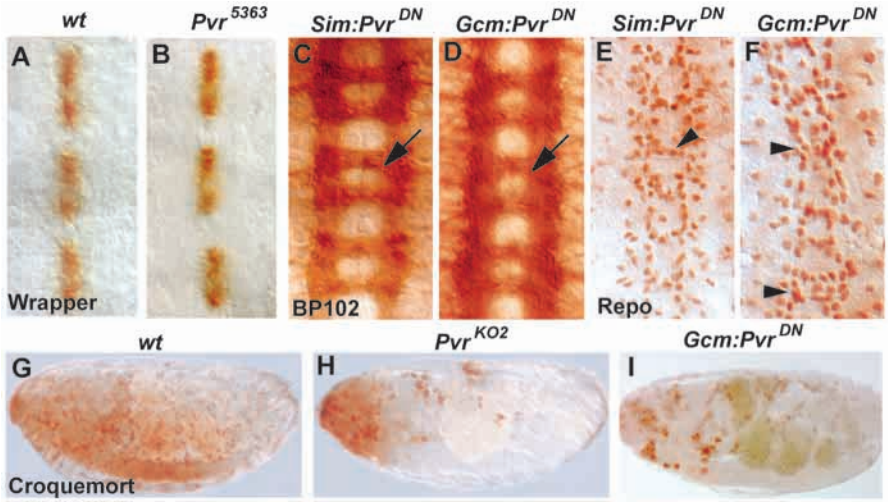

Fig. 5. *Pvr* acts in hemocytes and not midline glia for proper CNS patterning. (A,B) Stage 16 embryos stained with anti-wrapper antibody to visualize midline glia. Pvr^{5363} midline glia (B) are indistinguishable from wild type (A). (C,D) Stage 16 (C) *Sim-Gal4*;*UAS-*Pvr^{DN} and (D) *Gcm-Gal4*;*UAS-*Pvr^{DN} embryos stained with mAb BP102 to visualize CNS axons. *Sim-Gal4*;*UAS-*Pvr^{DN} embryos are indistinguishable from wild type, with commissures and longitudinal tracts forming a rectangular axon scaffold in each segment (arrow). *Gcm-Gal4*;*UAS-*Pvr^{DN} embryos resemble *Pvr* embryos, with the axon scaffold having a rounded appearance in each segment (arrow). (E,F) Stage 16 (E) *Sim-Gal4*;*UAS-*Pvr^{DN} and (F) *Gcm-Gal4*;*UAS-*Pvr^{DN} embryos stained with anti-Repo antibody to visualize glia. *Sim-Gal4*;*UAS-*Pvr^{DN} embryos have glia in normal positions, with only few glia located between commissures in each segment (arrowhead), while many segments of *Gcm-Gal4*;*UAS-*Pvr^{DN} embryos have clusters of glia near the midline (arrowheads). (G-I) Stage 16 (G) wild type (Canton-S), (H) Pvr^{KO2} and (I) *Gcm-Gal4*;*UAS-*Pvr^{DN} embryos stained with anti-Croquemort to visualize hemocytes. In wild type, hemocytes are dispersed throughout the embryo, while in *Pvr* mutants and *Gcm-Gal4*;*UAS-*Pvr^{DN} embryos hemocytes are largely clustered near the dorsal and anterior regions of the embryo. Anterior is towards the left and dorsal is towards the top.

Macrophage function is required for CNS patterning

To further examine the potential contribution of hemocytes to CNS development, we examined animals mutant for *serpent* (*srp*), which encodes a GATA-family transcription factor required for hemocyte development (Rehorn et al., 1996). srp^{neo45} is a hemocyte-specific allele of *serpent*, and srp^{neo45} animals lack all hemocytes (Lebestky et al., 2000; Rehorn et al., 1996). Examination of srp^{neo45} embryos demonstrated that not only did srp^{neo45} mutants lack macrophages, they also exhibited CNS axon scaffold defects similar to those in *Pvr* mutants, with characteristic rounding of commissures (Fig. 6C). Quantitative representation of CNS axon tract morphology in srp^{neo45} mutants confirmed this observation (Table 1). The ratio of the distance between the longitudinal axon tracts and the distance between the commissural axon tracts in srp^{neo45} mutants was significantly different from wild type ($P<0.01$), but not significantly different from *Pvr* homozygotes ($P>0.2$) (Table 1). srp^{neo45} animals also showed longitudinal glia positioning defects similar to those seen in *Pvr* mutants (Fig. 6G). Thus, mutants that disrupt either hemocyte production or migration cause similar alterations in CNS morphogenesis.

One possible explanation for dependence of CNS morphogenesis on hemocytes is that hemocyte-derived macrophages are needed to engulf cell corpses generated during development. To test this possibility we examined animals in which macrophages appear to develop normally, but fail to engulf cell corpses. This was achieved using animals with reduced function of *crq*, which encodes a CD36-related receptor required for *Drosophila* macrophages to engulf dead cells (Franc et al., 1999). Previous genetic studies of *crq* function used the chromosomal deficiencies *Df(2L)al* and *Df(2L)TE99(Z)XW88*. These deficiencies remove a number of genes, including *u-shaped*, a transcriptional regulator that acts in the hemocyte lineage and is involved in germ-band contraction (Fossett et al., 2001; Franc et al., 1999). As the elimination of multiple genes affecting potentially related processes complicates the use of *Df(2L)al* and *Df(2L)TE99(Z)XW88* in the analysis of CNS development, *crq* loss-of-function was examined using RNAi. Embryos injected with dsRNA corresponding to either of two non-overlapping regions within the Crq transcript had CNS axon scaffold defects similar to those in *Pvr* and *srp* mutants (Fig. 6D). In *crq* RNAi embryos the ratio of distance between longitudinals to distance between commissures was significantly different from wild type ($P<0.01$), but not significantly different from *Pvr* or *srp* mutants ($P>0.2$) (Table 1). In addition, *crq* RNAi animals also showed defects in the positioning of Repo-positive glia similar to those seen in *Pvr* and *srp* mutants (Fig. 6H). These data further support the importance of hemocytes in CNS morphogenesis and specifically suggest that engulfment of dead cells by hemocyte-derived macrophages is essential for CNS development.

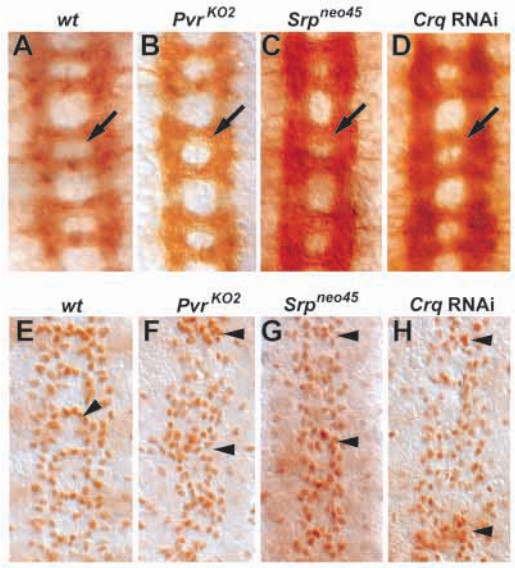

Fig. 6. Macrophage function is required for proper CNS patterning. (A-D) Stage 16 (A) wild type, (B) $Pvr^{KO2,}$, (C) Srp^{neo45} and (D) *Crq* RNAi embryos stained with BP102 to visualize CNS axons. Srp^{neo45} and *Crq* RNAi embryos resemble *Pvr* embryos, with the axon scaffold having a rounded appearance in each segment (arrows). (E-H) Stage 16 (E) wild type, (F) $Pvr^{KO2,}$, (G) Srp^{neo45} and (H) *Crq* RNAi embryos stained with Repo to visualize glia. Pvr^{KO2}, Srp^{neo45} and *Crq* RNAi embryos all have disruptions in the pattern of Repo-positive glia. Srp^{neo45} mutant embryos have increased numbers of Repo-positive glia at the midline in each segment (arrowheads). In *Crq* RNAi embryos, there are also increased numbers of glia at the midline (arrowheads), while the glia associated with longitudinal tracts appear more dispersed than in wild type (arrow).

DISCUSSION

We have examined the role of macrophage function in *Drosophila* development using several genetic approaches. Through a combination of site-specific gene targeting and chemical mutagenesis we generated and characterized a series of mutations in *Pvr*, which encodes a receptor tyrosine kinase of the PDGF/VEGF receptor family. In addition to disrupting macrophage migration, a function of *Pvr* recently described by Cho et al. (Cho et al., 2002), we find that *Pvr* mutants have defects in glial positioning and axon scaffold formation in the CNS. Tissue-specific expression of dominant-negative Pvr suggests that the CNS defects result from the disruption in macrophage positioning. Consistent with this interpretation, similar defects in CNS patterning are observed in animals that completely lack macrophages (srp^{neo45} mutants) and in animals in which expression of Croquemort (Crq), a receptor required for macrophage engulfment of dead cells, is inhibited. Taken together, these data suggest that macrophages play an important role in CNS development. Furthermore, as the effects on CNS morphogenesis of inhibiting *croquemort* function are essentially indistinguishable from eliminating macrophages altogether, our data suggest that corpse engulfment is a major aspect, and perhaps the most important aspect, of macrophage function in CNS development.

There are several possible explanations for the observed contribution of macrophages to CNS morphogenesis. As engulfment is capable of promoting cell death in some situations (Reddien et al., 2001), the inhibition of macrophage function could potentially change patterns of cell death. However, previous work found that substantial cell death still occurs in *Drosophila* embryos in the absence of macrophages (Tepass et al., 1994). Similarly, we find no alteration in the number of midline glia in *Pvr* mutants, suggesting that the

death of midline glia proceeds normally. Acridine Orange staining of developing embryos likewise shows no detectable alteration in the pattern of dead cell generation (H.C.S., C.J.K. and P.A.G., unpublished). Thus, although subtle changes in pattern of cell death would escape detection by these methods, there is no large-scale alteration in cell death in *Drosophila* in the absence of macrophages. Interestingly, when cell death is blocked in homozygous *Df(3L)H99* animals, which lack the cell death promoting genes *hid*, *grim* and *reaper*, the CNS axon scaffolds are wider than normal (Zhou et al., 1995) (H.C.S., C.J.K. and P.A.G., unpublished). The phenotypic contrast between the absence of cell death and the absence of macrophages suggests that macrophages are not simply required to remove material from the developing midline.

An alternative explanation for the need for macrophage-mediated engulfment is that the accumulation of cell corpses within the CNS disrupts axon and glial positioning. Cell corpses could exert a toxic effect or could disrupt the function of particular cell populations by abnormally accumulating within these cells. Such possibilities are consistent with Sonnenfeld and Jacobs' observation that in embryos from *Bic-D* mutant mothers (which, in addition to severe embryonic patterning defects, lack macrophages) cell corpses accumulate at the CNS periphery and in CNS glial cells (Sonnenfeld and Jacobs, 1995b). In the case of glial cells, it is interesting to note that the CNS defects of *Pvr*, *serpent*^{neo45} and *crq* RNAi animals resemble those of *repo* mutant animals in which glial positioning and survival is disrupted (Campbell et al., 1994; Halter et al., 1995). Thus, a disruption in glial positioning could lead to the disruption of the CNS axon scaffold observed in the absence of macrophage-mediated engulfment.

Another possible requirement for the engulfment of dead cells by macrophages could be that engulfment stimulates the release by macrophages of factors required for proper CNS morphogenesis. *Drosophila* macrophages produce extracellular matrix components such as collagen IV, laminin, papilin, glutactin and macrophage-derived proteoglycan-1 (MDP-1) (Fessler et al., 1994; Gullberg et al., 1994; Hortsch et al., 1998), and the presence of cell corpses is known to enhance production of at least one of these, MDP-1 (Hortsch et al., 1998). That *Pvr*, *serpent*^{neo45} and *crq* RNAi animals all show a mild elongation of the nerve cord (H.C.S., C.J.K. and P.A.G., unpublished) could reflect defects in extracellular matrix production.

Cell death is a major component of many morphogenetic processes during development in vertebrates and invertebrates. However, an essential role for macrophages in these morphogenetic events has been established only in the mouse retina, where macrophages appear to act by triggering cell death (Lang et al., 1994; Lang and Bishop, 1993). Unlike the mouse retina, cell death in the *Drosophila* CNS does not require macrophages (Tepass et al., 1994). Our data support a different role for macrophages in *Drosophila* CNS morphogenesis: mediating clearance of dead cells. These observations indicate that both cell death and the interaction of macrophages with cell corpses are required for proper *Drosophila* CNS development.

We thank C. Thomas and M. Robichaux for technical assistance; U. Banerjee, P. Duchek, R. Ezekowitz, J. Fessler, L. Fessler, K. Golic, C. Goodman, Y. Rong, P. Rorth, J. Simpson, U. Tepass and the Developmental Studies Hybridoma Bank for antibodies and fly stocks; and A. Chess, N. Franc, H. R. Horvitz, L. Huang, E. Nedivi, T. Orr-Weaver, S. L. Zipursky and Garrity laboratory members for discussions. This work was supported by grants to P.A.G. from the National Institutes of Health (1RO1EY/MH13874-01), the Raymond and Beverly Sackler Foundation, the Leukemia and Lymphoma Society, and the McKnight Foundation. H.C.S. is supported by a Centocor Fellowship. P.A.G. is an investigator and C.J.K. is a research associate of the Raymond and Beverly Sackler Foundation.

REFERENCES

Abrams, J. M. (2002). Competition and compensation: coupled to death in development and cancer. *Cell* **110**, 403-406.

Baehrecke, E. H. (2002). How death shapes life during development. *Nat. Rev. Mol. Cell Biol.* **3**, 779-787.

Bangs, P. and White, K. (2000). Regulation and execution of apoptosis during Drosophila development. *Dev. Dyn.* **218**, 68-79.

Bello, B. C., Hirth, F. and Gould, A. P. (2003). A pulse of the *Drosophila* Hox protein abdominal-A schedules the Endo of neural proliferatin via neuroblast apoptosis. *Neuron* **37**, 209-219.

Bergmann, A., Tugentman, M., Shilo, B. Z. and Steller, H. (2002). Regulation of cell number by MAPK-dependent control of apoptosis: a mechanism for trophic survival signaling. *Dev. Cell* **2**, 159-170.

Campbell, G., Goring, H., Lin, T., Spana, E., Andersson, S., Doe, C. Q. and Tomlinson, A. (1994). RK2, a glial-specific homeodomain protein required for embryonic nerve cord condensation and viability in Drosophila. *Development* **120**, 2957-2966.

Cho, N. K., Keyes, L., Johnson, E., Heller, J., Ryner, L., Karim, F. and Krasnow, M. A. (2002). Developmental control of blood cell migration by the Drosophila VEGF pathway. *Cell* **108**, 865-876.

Duchek, P. and Rorth, P. (2001). Guidance of cell migration by EGF receptor signaling during drosophila oogenesis. *Science* **291**, 131-133.

Duchek, P., Somogyi, K., Jekely, G., Beccari, S. and Rorth, P. (2001). Guidance of cell migration by the Drosophila PDGF/VEGF receptor. *Cell* **107**, 17-26.

Fadok, V. A. and Chimini, G. (2001). The phagocytosis of apoptotic cells. *Semin. Immunol.* **13**, 365-372.

Fessler, L. I., Nelson, R. E. and Fessler, J. H. (1994). Drosophila extracellular matrix. *Methods Enzymol.* **245**, 271-294.

Fossett, N., Tevosian, S. G., Gajewski, K., Zhang, Q., Orkin, S. H. and Schulz, R. A. (2001). The friend of GATA proteins U-shaped, FOG-1, and FOG-2 function as negative regulators of blood, heart, and eye development in Drosophila. *Proc. Natl. Acad. Sci. USA* **98**, 7342-7347.

Franc, N. C. (2002). Phagocytosis of apoptotic cells in mammals, caenorhabditis elegans and Drosophila melanogaster: molecular mechanisms and physiological consequences. *Front Biosci.* **7**, D1298-1313.

Franc, N. C., Dimarcq, J. L., Lagueux, M., Hoffmann, J. and Ezekowitz, R. A. (1996). Croquemort, a novel Drosophila hemocyte/macrophage receptor that recognizes apoptotic cells. *Immunity* **4**, 431-443.

Franc, N. C., Heitzler, P., Ezekowitz, R. A. and White, K. (1999). Requirement for croquemort in phagocytosis of apoptotic cells in Drosophila. *Science* **284**, 1991-1994.

Gullberg, D., Fessler, L. I. and Fessler, J. H. (1994). Differentiation, extracellular matrix synthesis, and integrin assembly by Drosophila embryo cells cultured on vitronectin and laminin substrates. *Dev. Dyn.* **199**, 116-128.

Halter, D. A., Urban, J., Rickert, C., Ner, S. S., Ito, K., Travers, A. A. and Technau, G. M. (1995). The homeobox gene repo is required for the differentiation and maintenance of glia function in the embryonic nervous system of Drosophila melanogaster. *Development* **121**, 317-332.

Hanks, S. K., Quinn, A. M. and Hunter, T. (1988). The protein kinase family: conserved features and deduced phylogeny of the catalytic domains. *Science* **241**, 42-52.

Heino, T. I., Karpanen, T., Wahlstrom, G., Pulkkinen, M., Eriksson, U., Alitalo, K. and Roos, C. (2001). The Drosophila VEGF receptor homolog is expressed in hemocytes. *Mech. Dev.* **109**, 69-77.

Hidalgo, A. and Booth, G. E. (2000a). Glia dictate pioneer axon trajectories in the Drosophila embryonic CNS. *Development* **127**, 393-402.

Hidalgo, A. and Booth, G. E. (2000b). Glia dictate pioneer axon trajectories in the Drosophila embryonic CNS. *Development* **127**, 393-402.

Hidalgo, A. and Brand, A. H. (1997). Targeted neuronal ablation: the role of

pioneer neurons in guidance and fasciculation in the CNS of Drosophila. *Development* **124**, 3253-3262.

Hidalgo, A., Kinrade, E. F. and Georgiou, M. (2001). The Drosophila neuregulin vein maintains glial survival during axon guidance in the CNS. *Dev. Cell* **1**, 679-690.

Hopkinson-Woolley, J., Hughes, D., Gordon, S. and Martin, P. (1994). Macrophage recruitment during limb development and wound healing in the embryonic and foetal mouse. *J. Cell Sci.* **107**, 1159-1167.

Hortsch, M., Olson, A., Fishman, S., Soneral, S. N., Marikar, Y., Dong, R. and Jacobs, J. R. (1998). The expression of MDP-1, a component of Drosophila embryonic basement membranes, is modulated by apoptotic cell death. *Int. J. Dev. Biol.* **42**, 33-42.

Huang, Z., Shilo, B. Z. and Kunes, S. (1998). A retinal axon fascicle uses spitz, an EGF receptor ligand, to construct a synaptic cartridge in the brain of Drosophila. *Cell* **95**, 693-703.

Hume, D. A., Perry, V. H. and Gordon, S. (1983). Immunohistochemical localization of a macrophage-specific antigen in developing mouse retina: phagocytosis of dying neurons and differentiation of microglial cells to form a regular array in the plexiform layers. *J. Cell Biol.* **97**, 253-257.

Jacobs, J. R. (2000). The midline glia of Drosophila: a molecular genetic model for the developmental functions of glia. *Prog. Neurobiol.* **62**, 475-508.

Jacobs, J. R. and Goodman, C. S. (1989). Embryonic development of axon pathways in the Drosophila CNS. I. A glial scaffold appears before the first growth cones. *J. Neurosci.* **9**, 2402-2411.

Jacobson, M. D., Weil, M. and Raff, M. C. (1997). Programmed cell death in animal development. *Cell* **88**, 347-354.

Jiang, C., Baehrecke, E. H. and Thummel, C. S. (1997). Steroid regulated programmed cell death during Drosophila metamorphosis. *Development* **124**, 4673-4683.

Johnson, L. N., Noble, M. E. and Owen, D. J. (1996). Active and inactive protein kinases: structural basis for regulation. *Cell* **85**, 149-158.

Kennerdell, J. R. and Carthew, R. W. (1998). Use of dsRNA-mediated genetic interference to demonstrate that frizzled and frizzled 2 act in the wingless pathway. *Cell* **95**, 1017-1026.

Kidd, T., Bland, K. S. and Goodman, C. S. (1999). Slit is the midline repellent for the robo receptor in Drosophila. *Cell* **96**, 785-794.

Kidd, T., Brose, K., Mitchell, K. J., Fetter, R. D., Tessier-Lavigne, M., Goodman, C. S. and Tear, G. (1998). Roundabout controls axon crossing of the CNS midline and defines a novel subfamily of evolutionarily conserved guidance receptors. *Cell* **92**, 205-215.

Klambt, C., Jacobs, J. R. and Goodman, C. S. (1991). The midline of the Drosophila central nervous system: a model for the genetic analysis of cell fate, cell migration, and growth cone guidance. *Cell* **64**, 801-815.

Lang, R., Lustig, M., Francois, F., Sellinger, M. and Plesken, H. (1994). Apoptosis during macrophage-dependent ocular tissue remodelling. *Development* **120**, 3395-3403.

Lang, R. A. and Bishop, J. M. (1993). Macrophages are required for cell death and tissue remodeling in the developing mouse eye. *Cell* **74**, 453-462.

Lebestky, T., Chang, T., Hartenstein, V. and Banerjee, U. (2000). Specification of Drosophila hematopoietic lineage by conserved transcription factors. *Science* **288**, 146-149.

Lin, D. M., Fetter, R. D., Kopczynski, C., Grenningloh, G. and Goodman, C. S. (1994). Genetic analysis of Fasciclin II in Drosophila: defasciculation, refasciculation, and altered fasciculation. *Neuron* **13**, 1055-1069.

Lohmann, I., McGinnis, N., Bodmer, M. and McGinnis, W. (2002). The Drosophila Hox gene deformed sculpts head morphology via direct regulation of the apoptosis activator reaper. *Cell* **110**, 457-466.

Morris, L., Graham, C. F. and Gordon, S. (1991). Macrophages in haemopoietic and other tissues of the developing mouse detected by the monoclonal antibody F4/80. *Development* **112**, 517-526.

Nambu, J. R., Lewis, J. O., Wharton, K. A., Jr and Crews, S. T. (1991). The Drosophila single-minded gene encodes a helix-loop-helix protein that acts as a master regulator of CNS midline development. *Cell* **67**, 1157-1167.

Nelson, R. E., Fessler, L. I., Takagi, Y., Blumberg, B., Keene, D. R., Olson, P. F., Parker, C. G. and Fessler, J. H. (1994). Peroxidasin: a novel enzyme-matrix protein of Drosophila development. *EMBO J.* **13**, 3438-3447.

Noordermeer, J. N., Kopczynski, C. C., Fetter, R. D., Bland, K. S., Chen, W. Y. and Goodman, C. S. (1998). Wrapper, a novel member of the Ig superfamily, is expressed by midline glia and is required for them to ensheath commissural axons in Drosphila. *Neuron* **21**, 991-1001.

Patel, N. H. (1994). Imaging neuronal subsets and other cell types in whole-mount *Drosophila* embryos and larvae using antibody probes. In *Methods in Cell Biology*, Vol. 44 (ed. E. A. Fyrberg), pp. 445-487. San Diego: Academic Press.

Reddien, P. W., Cameron, S. and Horvitz, H. R. (2001). Phagocytosis promotes programmed cell death in C. elegans. *Nature* **412**, 198-202.

Rehorn, K. P., Thelen, H., Michelson, A. M. and Reuter, R. (1996). A molecular aspect of hematopoiesis and endoderm development common to vertebrates and Drosophila. *Development* **122**, 4023-4031.

Rong, Y. S. and Golic, K. G. (2000). Gene targeting by homologous recombination in Drosophila. *Science* **288**, 2013-2018.

Rong, Y. S. and Golic, K. G. (2001). A targeted gene knockout in drosophila. *Genetics* **157**, 1307-1312.

Sonnenfeld, M. J. and Jacobs, J. R. (1995a). Apoptosis of the midline glia during Drosophila embryogenesis: a correlation with axon contact. *Development* **121**, 569-578.

Sonnenfeld, M. J. and Jacobs, J. R. (1995b). Macrophages and glia participate in the removal of apoptotic neurons from the Drosophila embryonic nervous system. *J. Comp. Neurol.* **359**, 644-652.

Tepass, U., Fessler, L. I., Aziz, A. and Hartenstein, V. (1994). Embryonic origin of hemocytes and their relationship to cell death in Drosophila. *Development* **120**, 1829-1837.

Van Vactor, D. V., Sink, H., Fambrough, D., Tsoo, R. and Goodman, C. S. (1993). Genes that control neuromuscular specificity in *Drosophila*. *Cell* **73**, 1137-1153.

Wood, W., Turmaine, M., Weber, R., Camp, V., Maki, R. A., McKercher, S. R. and Martin, P. (2000). Mesenchymal cells engulf and clear apoptotic footplate cells in macrophageless PU.1 null mouse embryos. *Development* **127**, 5245-5252.

Zhou, L., Hashimi, H., Schwartz, L. M. and Nambu, J. R. (1995). Programmed cell death in the Drosophila central nervous system midline. *Curr. Biol.* **5**, 784-790.